Design and construction of a continuous impregnation apparatus of woven fibres, using non-meshing double-sinusoidal toothed rollers

G. Vasileiou[1*], C. Vakouftsis[1], N. Rogkas[1], S. Tsolakis[1], P. Zalimidis[2], V. Spitas[1]

[1]School of Mechanical Engineering, National Technical University of Athens – NTUA
[2]Department of Mechanical Engineering Educators, School of Pedagogical and Technological Education – ASPETE

Abstract. Resin-impregnated fibres are extensively used in a variety of industrial applications as is demonstrated in the literature. Resin-fibre impregnation techniques are used in order to create homogeneous macro – materials and to take full advantage of the mechanical properties of the fibrous reinforcement (i.e. carbon, glass, organic or ceramic fibres). However, achieving highly impregnated fibres is proven quite challenging especially in continuous production techniques that are required for large production rates. The main challenge lies in achieving complete impregnation of the tightly arranged fibres mainly referring to the formed yarns containing multiple fibres, sometimes even twisted. This results in partially impregnated materials containing cavities that tend to exhibit inferior mechanical properties compared to the theoretical calculations, which assume fully impregnated materials. These cavities often lead to crack generation, acting as stress concentration sites, resulting in complete failure of the material at macro-level. In this paper a novel technique for continuous production of fully impregnated woven fibres is presented using non – meshing, co – rotating rollers. A laboratory-scale apparatus is designed and described thoroughly in the context of this work. The method resembles pultrusion in the sense that a reinforcement plain fibre mesh (glass) is co–processed with the liquid resin through a pair of co–rotating toothed rollers to produce a continuously reinforced 3D tape. The surface of the rollers is produced from a double-sinusoidal toothed surface (rack) using the Theory of Gearing in three-dimensions, which imposes significant differential sliding of the fibres without differential tension and facilitates fibre wetting. The geometry of the rollers is calculated not to damage the unprocessed fibres, while facilitating local widespreading of the stranded fibres in the three – dimensional space leading to the resin being able to fully penetrate the reinforcing fibre material.

1 Introduction

Fibre reinforced polymers are used extensively in various industrial applications such as single layer flexible composites, multi-layer composite panels, sandwich panels combined with metallic cores, single-or multi-directional fibre reinforcements and auxetic behaviour layout fibre reinforcements among others [1-7]. Due to the extensive range of applications, fibre reinforced polymers may include either stiff elements used in structural applications [8, 9] or flexible composites used in high end applications [10, 11]. Modern techniques such as 3D printing has been incorporated recently in the production of continuous fibre reinforced polymers [12, 13]. Achieving high level of impregnation through the usually tightly stranded fibres is the most challenging task in continuous fibre production techniques that are required for large production rates since the impregnation levels dictate the resulting composite material strength compared to the theoretical values occurring from predetermining the volume ratios of the reinforcement material to the core material. Imperfect impregnation may result in the creation of cavities inside the resin/ polymeric core that may in turn act as stress concentration and therefore crack initiation faults. Lekakou et al. [14] investigated the permeability of woven fibres during the resin transfer (RTM) molding process, while multiple works have studied the various molding and production techniques of fibre reinforced composites, namely Williams et al. [15] who studied the resin infusion under flexible tooling (RIFT) production method, Sas et al. [16] who proposed optimization tools for high resin impregnation during a variation of the Vacuum Assisted Resin Transfer Molding (VARTM), Schechter et al. [17] who proposed a dewetting process that can allow for higher permeability in fibre reinforced resins and also investigated ways to remove air trapped in the composites during the manufacturing process to improve permeability and overall mechanical

* Corresponding author: gvasileiou@mail.ntua.gr

properties [18], Reddy et al. [19] who performed a full analysis of woven fibre reinforced composites including fabrication, testing and evaluation techniques, Kim et al. [20] who investigated the directional permeability of woven fabric reinforcements and Lekakou et al. [21] who proposed a modelling method for calculating the infiltration in macro and micro level in the RTM technique.
In the context of this paper, a novel technique is presented to produce flexible woven cloth reinforced polymeric resins through a continuous production described in detail. The concept of non-meshing, co-rotating gears is introduced and analyzed, contrary to the conventional technique that incorporates squeezing of the woven tape through simple cylindrical rollers. The purpose of the gears is to induce differential sliding on the tightly stranded woven cloth fibres and therefore creating the empty space required for the resin to impregnate the cloth, while no tensile loads act on the fibres. An experimental laboratory scale test rig is designed and presented throughout the presented work in order to produce prototype specimens and test the resin penetration among the glass fibre of the woven tape. Moreover, rapid prototyping techniques are investigated and evaluated for the production on the gears that consist of double sinusoidal form produced from the three dimensional Theory of Gearing. Finally, the novelty of the proposed method is further enhanced by the fact that the calculated improvement in the impregnation of the woven fibres is almost 30% compared to conventional cylindrical rollers.

2 Toothed roller design

The design of the rollers is based on two crucial parameters namely high fibre impregnation efficiency and minimum fibre damage before and during the impregnation.

The geometry of the roller is a double-sinusoidal toothed surface. The equation of the sinusoidal surface of the rack that produces the toothed rollers is given by Eq. 1.

$$z(x,y) = A_x sin\left(\frac{2\pi}{l_x}x + \varphi_x\right) + A_y sin\left(\frac{2\pi}{l_y}y + \varphi_y\right) \quad (1)$$

In order to achieve symmetrical tooth design and extension of the fabric fibres, the amplitude A as well as the pitch l of the sinusoidal functions are set equal and Eq. 1 is therefore transformed in Eq. 2.

$$z(x,y) = A\left(sin\left(\frac{2\pi}{l}x\right) + sin\left(\frac{2\pi}{l}y\right)\right) \quad (2)$$

Since Eq. 2 describes the geometry of the rack shown in Fig. 1, it is possible to design the toothed rollers through application of the three dimensional Theory of Gearing. Estimation of the amplitude (A), and the pitch (l) of the rack form given by Eq. 1 will provide all the necessary data for the design of the toothed rollers.

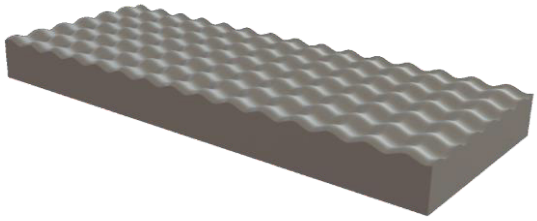

Fig. 1. Solid model of the rack.

The pitch (l) of the sinusoidal rack form is going to be the same as the circular pitch of the toothed rollers at the pitch circle. The circular pitch (t) of the toothed roller is given by Eq. 3.

$$t = \frac{2\pi r_0}{Z} \quad (3)$$

Substituting Eq. 3 to Eq. 2 the rack geometry is expressed in terms used by the Theory of Gearing as shown in Eq. 4.

$$z(x,y) = A\left(sin\left(\frac{Z}{r_0}x\right) + sin\left(\frac{Z}{r_0}y\right)\right), \quad (4)$$

where Z is the number of teeth.
Therefore, design of the toothed rollers is subject to determining the amplitude (A), the number of teeth (Z) and the radius of the pitch circle.

2.1 Modelling

In order to calculate the dimensions of the toothed rollers the improvement in the resulting impregnation as well as torque requirements are calculated parametrically for gears with *Z=20* teeth. The parameters used are the tape velocity (*v*), the roller pitch circle radius (r_0) and the total tooth height (*h*). The results are shown in Figures 2, 3a and 3b.

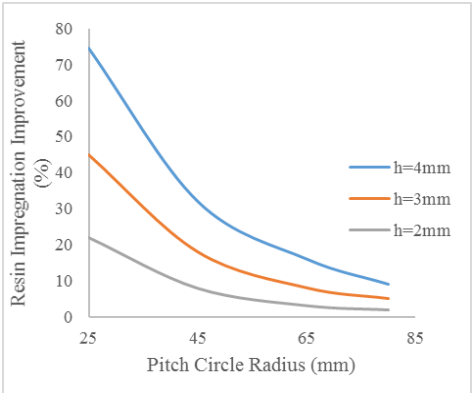

Fig. 2. Resin improvement percentage versus tooth height and pitch circle radius for tape velocity *v=0.1m/s*.

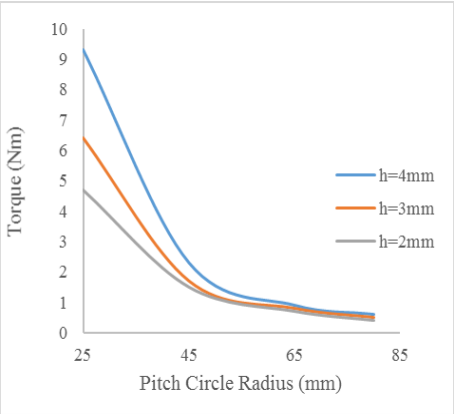

Fig. 3a. Torque versus tooth height and pitch circle radius for tape velocity *v=0.05m/s*.

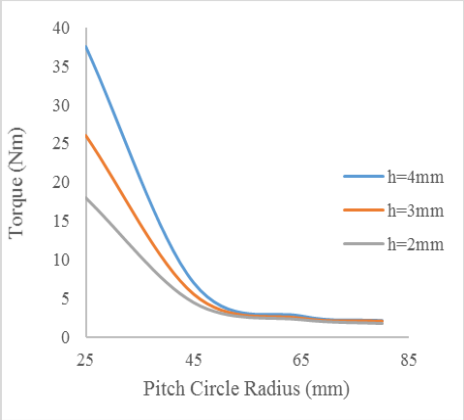

Fig. 3b. Torque versus tooth height and pitch circle radius for tape velocity *v=0.1m/s*.

Figure 2 shows the dependency of the resin impregnation improvement versus the geometrical characteristics of the gear rollers for tape velocity *v=0.1m/s*. Tape velocity *v=0.05m/s* is not shown since the results show negligible deviations compared to the *v=0.1m/s* tape velocity (deviations less than 10^{-1}). Figures 3a and 3b show the resulting torque on the toothed rollers. Therefore, tape velocity was set at *v=0.1m/s,* the height of the teeth was selected at *h=3mm* and the roller pitch circle radius was set at r_0*=32mm*. The total tooth height (h) is twice the amplitude (A) of each sinusoidal term of Eq. 4. The final geometry of the rack that produces the toothed rollers is shown in Fig. 4.

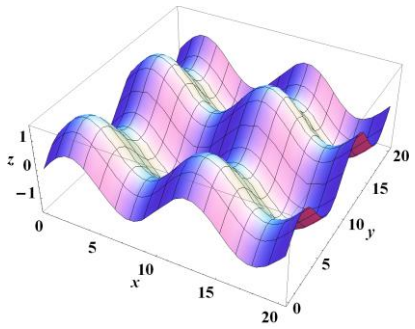

Fig. 4. Final geometry of the double-sinusoidal rack.

Since the geometrical characteristics of the rack are defined the toothed rollers can be designed through the Theory of Gearing in three dimensions. Table 1 contains the full geometrical characteristics of the resulting toothed roller geometry. Finally, due to the elaborate surface geometry of the toothed rollers, the prototypes were constructed using rapid prototyping techniques (3D printing) as discussed in detail in section 3 of the present work. The final geometry of the toothed rollers is shown in Fig. 5.

Table 1. Toothed roller characteristics.

Number of teeth	Z=20
Tooth height	h=3mm
Amplitude of the double sinusoidal rack geometry function	2*A=1,5mm
Pitch circle radius	r_0 = 32mm
Pitch	t=10,053mm
Material	ABS Plastic
Inner Diameter	55mm
Width (six pitches)	60,32mm
Weight	50,45 gr

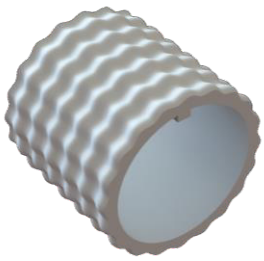

Fig. 5. Model of the double-sinusoidal toothed roller.

The glass fibre tape thickness is estimated by the manufacturer at 0.34mm. Therefore, the toothed rollers are not positioned in the nominal centre distance ($a_{0,nom}$=64mm) but at $a_{0,act}$=64.34mm instead.

3 Prototyping & experimental evaluation

In order to evaluate the analysis presented earlier, a laboratory scale test rig is designed and used for testing of the operation of the toothed rollers.

3.1 Construction of the toothed roller prototypes

As stated earlier in the presented work, the complex geometry of the toothed rollers, derived from the double-sinusoidal form of the rack, would require expensive 4-axis CNC milling in order to produce using conventional material removal production methods. On the other hand, additive manufacturing (AM) is becoming increasingly popular as a manufacturing process for fast producing working prototypes, especially for complex shapes and free forms that conventional manufacturing processes are unable or expensive to produce.
Therefore, the construction of the prototype toothed rollers was performed using the 3D printing FDM technique. The fabrication of the prototypes was performed using Stratasys Fortus 360mc 3D printer of the Rapid Prototyping and Tooling (RP&T) Laboratory of NTUA's School of Mechanical Engineering. The aforementioned printer uses FDM technology and ABS plus (P430) as building material with a building envelope of 355 × 254 × 254 mm. Due to the design of the roller the optimal building direction is perpendicular to the axis of the cylinder, in order to minimize support structure, time and building cost as shown in Fig. 6.

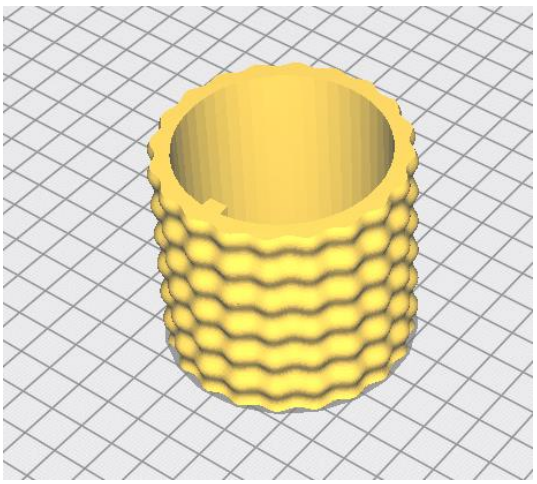

Fig. 6. Building direction of roller.

Dimensional accuracy of a 3D printed part depends on many parameters such as material, building direction, supports structure and layer height among others. One of the most crucial parameter for dimensional and geometrical accuracy is thermal history (thermal distribution during fabrication and cooling rates) of the part. By maintaining a constant temperature during fabrication and controlling the cooling rates of the fabricated part it is possible to minimize deviations. Thus due to the fact that Fortus 360mc has an embodied closed heated building chamber, minimal distortions and dimensional deviations are expected. The printed prototypes are shown in Fig. 7.

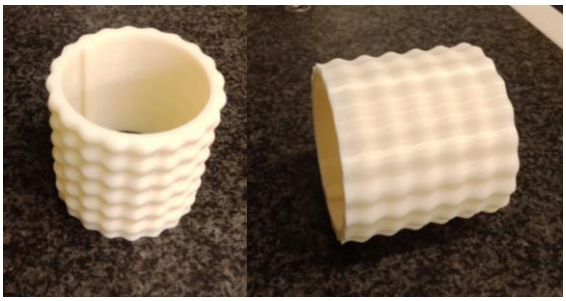

Fig. 7. 3D Printed toothed roller prototypes.

3.2 Evaluation of the toothed roller prototype accuracy

In order to evaluate the dimensional and geometrical accuracy of the manufactured geometry of the roller, measurements should be made and compare to the nominal dimensions. The evaluation process was performed using the portable robotic arm CMM of RP&T Laboratory of NTUA. The measurement scheme included both measurements taken using a touch probe of the robotic arm CMM as well as laser scanning using the same robotic arm CMM. Probe measurements are used for higher measurement accuracy in the points of interest, while laser scanning is preferable for obtaining the cloud points and evaluate the complete free form surface accuracy, through comparison with the CAD model that includes the nominal dimensions. Figures 8 and 9 shown the actual measurements of the prototype toothed roller. Processing of the point cloud was performed using Geomagic Qualify 2013 for the creation of the CAD model. Figure 10 shows the point cloud of the laser-scanned prototype toothed roller.

Fig. 8. Measurement of the toothed roller using the probe.

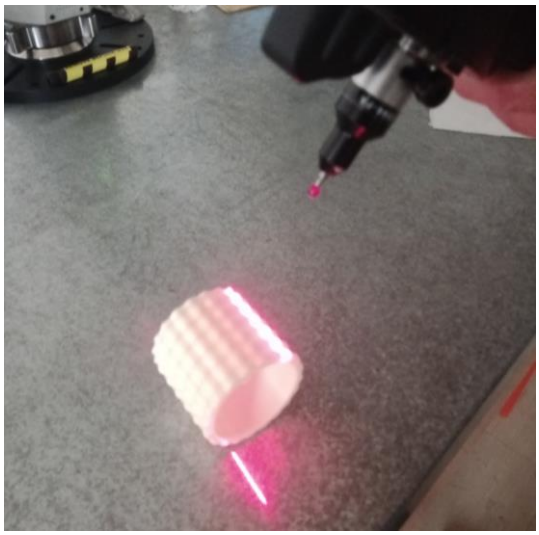

Fig. 9. Laser scanning of the roller.

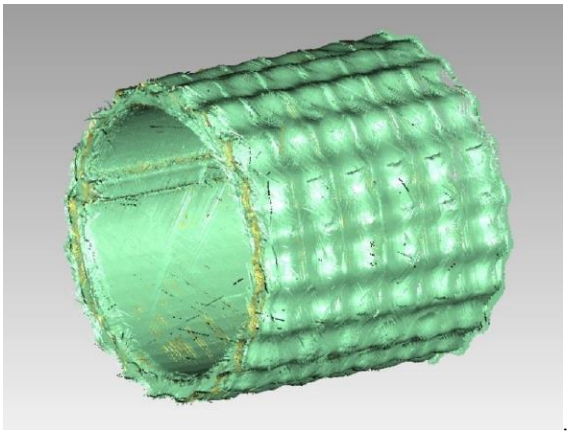

Fig. 10. Point cloud obtained by the laser scanner.

The model that was created by the post-processing of the point cloud obtained be the laser scanning was then compared with the nominal geometry model of the roller to determine the dimensional and shape deviations as shown in Fig. 11.

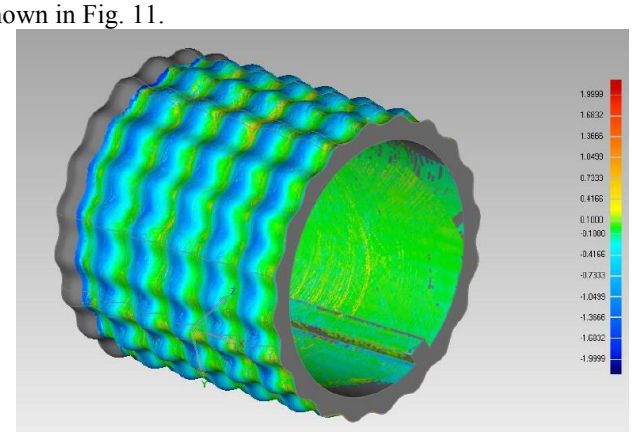

Fig. 11. Comparison of nominal and scanned model.

From this comparison it emerged that the deviation in the inner diameter of the wheel is observed to be smaller than 0.2mm. Also on the outer surface of the wheel it is observed that there has been a normalization of the waveform. More specifically, it seems that the height of the heads of the teeth has been reduced while at the same time their foot height has been reduced to around 0, 5mm. The measured deviations are significant compared to the height of the waveform, however, since similar data were obtained from both rollers, no interference occurs and the rollers can be tested normally.

3.3 Prototype test apparatus

For the experimental testing of the procedure a test rig for continues impregnation of woven fibres was manufactured. The 3D printed toothed rollers were assembled to metal mounts and then to the main shafts creating the forming pair of rollers.

Fig. 12. Assembly of 3D printed rollers with mounts.

Two pairs of plain cylindrical rollers were used as guides for the alignment of the fibres. After the forming of the fibre a pair of plain cylindrical rollers was used for re-forming the impregnated fibre into its final form by removing the remaining waviness induced by the geometry of the form rollers.

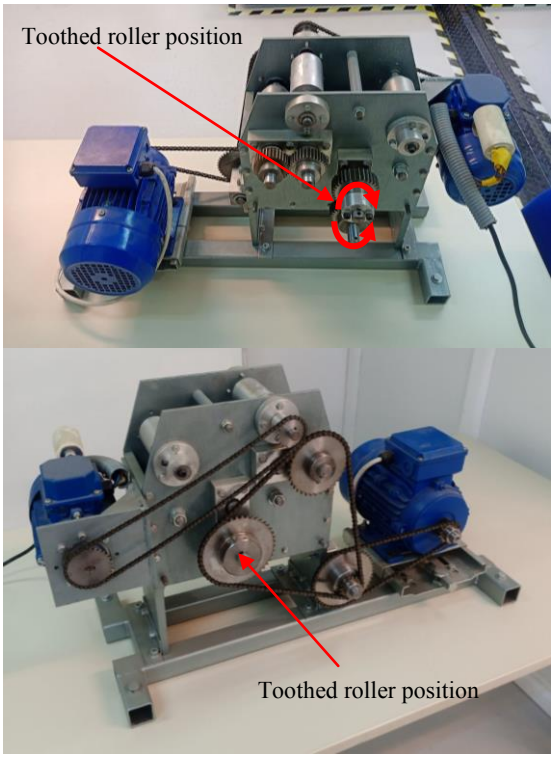

Fig. 13. Experimental testing rig.

4 Results and discussion

A novel method for continuous wetting of woven fibres incorporating double-sinusoidal toothed rollers as a replacement for conventional cylindrical ones was presented and discussed in detail throughout this work. Fabrication of the toothed rollers using modern, low-cost production methods is also presented and evaluated along with the construction of a laboratory scale test apparatus for performing evaluation testing on the proposed method.

Early experimental results shown in Fig. 14 shown the microscopic structure of the glass fibre reinforced resin produced using the toothed rollers versus conventional cylindrical rollers. The microscope taken photographs shown section view of the impregnated woven tape. The photographs are taken with a magnification factor of 200x. The red circles in Fig. 14 show packed fibres that haven't been impregnated with the resin. The improvement in the impregnation is calculated around 25% lower than the estimated 30%. This deviation is attributed to the form deviations in the outer surface of the toothed rollers.

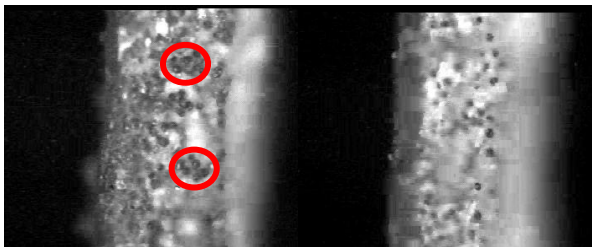

Fig. 14. Section view on the impregnated glass fibre tape produced by cylindrical rollers (left) versus toothed rollers (right). Photo taken from microscope.

The method has exhibited promising results during the early stages of laboratory scale applications and testing. This indicates that further development could enhance its performance and impregnation improvement. Future work includes the incorporation of optimisation tools for the determination of the toothed gear geometry as well as determination of the optimized parameters for the production of the toothed rollers using additive manufacturing techniques.
Finally, scaling up of the method could also be performed and investigated for application in high productivity industrial applications.

References

1. Kwietniewski, M., & Miedzińska, D. (2019). Review of Elastomeric Materials for Application to Composites Reinforced by Auxetics Fabrics. *Procedia Structural Integrity*, ***17***, 154-161.
2. Ramnath, B. V., Alagarraja, K., & Elanchezhian, C. (2019). Review on Sandwich Composite and their Applications. *Materials Today: Proceedings*, ***16***, 859-864.
3. Tian, Z., Liu, Y., Jiang, L., Zhu, W., & Ma, Y. (2019). A review on application of composite truss bridges composed of hollow structural section members. *Journal of Traffic and Transportation Engineering (English Edition)*, ***6*(1)**, 94-108.
4. Kushwaha, S., & Bagha, A. K. (2020). Application of composite materials for vibroacoustic–A review. *Materials Today: Proceedings*.
5. Yusuf, M., Kumar, M., Khan, M. A., Sillanpa, M., & Arafat, H. (2019). A review on exfoliation, characterization, environmental and energy applications of graphene and graphene-based composites. *Advances in colloid and interface science*, 102036.
6. Ayranci, C., & Carey, J. (2008). 2D braided composites: a review for stiffness critical applications. *Composite Structures*, ***85*(1)**, 43-58.
7. Zabihi, O., Ahmadi, M., Nikafshar, S., Preyeswary, K. C., & Naebe, M. (2018). A technical review on epoxy-clay nanocomposites: Structure, properties, and their applications in fiber reinforced composites. *Composites Part B: Engineering*, ***135***, 1-24.
8. Al-saadi, A. U., Aravinthan, T., & Lokuge, W. (2018). Structural applications of fibre reinforced polymer (FRP) composite tubes: A review of columns members. *Composite Structures*, ***204***, 513-524.
9. Correia, J. R., Bai, Y., & Keller, T. (2015). A review of the fire behaviour of pultruded GFRP structural profiles for civil engineering applications. *Composite Structures*, ***127***, 267-287.
10. Yang, S., Sun, L., An, X., & Qian, X. (2020). Construction of flexible electrodes based on ternary polypyrrole@ cobalt oxyhydroxide/cellulose fiber composite for supercapacitor. *Carbohydrate Polymers*, ***229***, 115455.
11. Zhang, C., Gong, J., Li, H., & Zhang, J. (2020). Fiber-based flexible composite with dual-gradient structure for sound insulation. *Composites Part B: Engineering*, 108166.
12. Anwer, A., & Naguib, H. E. (2018). Multi-functional flexible carbon fiber composites with controlled fiber alignment using additive manufacturing. *Additive Manufacturing*, ***22***, 360-367.
13. Davoodi, E., Fayazfar, H., Liravi, F., Jabari, E., & Toyserkani, E. (2020). Drop-on-demand high-speed 3D printing of flexible milled carbon fiber/silicone composite sensors for wearable biomonitoring devices. *Additive Manufacturing*, ***32***, 101016.
14. Lekakou, C., Johari, M. A. K., Norman, D., & Bader, M. G. (1996). Measurement techniques and effects on in-plane permeability of woven cloths in resin transfer moulding. Composites Part A: Applied Science and Manufacturing, **27(5)**, 401-408.
15. Williams, C., Summerscales, J., & Grove, S. (1996). Resin infusion under flexible tooling (RIFT): a

review. *Composites Part A: Applied Science and Manufacturing*, ***27*****(7)**, 517-524.

16. Sas, H. S., Šimáček, P., & Advani, S. G. (2015). A methodology to reduce variability during vacuum infusion with optimized design of distribution media. *Composites Part A: Applied Science and Manufacturing*, ***78***, 223-233.
17. Schechter, S. G., Centea, T., & Nutt, S. R. (2018). Polymer film dewetting for fabrication of out-of-autoclave prepreg with high through-thickness permeability. *Composites Part A: Applied Science and Manufacturing*, ***114***, 86-96.
18. Schechter, S. G., Centea, T., & Nutt, S. (2020). Effects of resin distribution patterns on through-thickness air removal in vacuum-bag-only prepregs. *Composites Part A: Applied Science and Manufacturing*, ***130***, 105723.
19. Reddy, B., & Narayana, K. B. (2018). Fabrication, testing and evaluation of mechanical properties of woven glass fibre composite material. *Materials Today: Proceedings*, ***5*****(1)**, 2429-2434.
20. Kim, J. I., Hwang, Y. T., Choi, K. H., Kim, H. J., & Kim, H. S. (2019). Prediction of the vacuum assisted resin transfer molding (VARTM) process considering the directional permeability of sheared woven fabric. *Composite Structures*, ***211***, 236-243.
21. Lekakou, C., & Bader, M. G. (1998). Mathematical modelling of macro-and micro-infiltration in resin transfer moulding (RTM). *Composites Part A: Applied Science and Manufacturing*, ***29*****(1-2)**, 29-37.